Chapter II.7

Cryogenics for superconducting devices

Philippe Lebrun
European Scientific Institute (ESI), Archamps, France
CERN retired, Geneva, Switzerland

This introduction to cryogenics focuses on the aspects of low-temperature science and technology applicable to the cooling of superconducting devices: properties of cryogenic fluids (helium and nitrogen) as compared to solid materials, refrigeration and liquefaction, heat transfer and thermal insulation, and use of cold vapour for thermal screening in cryostats and ancillaries such as current leads.

II.7.1 Introduction

Cryogenics is conventionally defined as the science and technology of low temperatures up to 120 K, thus encompassing the normal boiling points of the so-called "non-condensable" gases, i.e. those that cannot be liquefied by sheer compression at room temperature (see Table II.7.1). On a practical standpoint, this definition includes methane, the main component of liquid natural gas that constitutes, together with liquid air gases, the largest industrial application of cryogenics.

Table II.7.1: Characteristic temperatures of cryogens (K).

Cryogen	Triple point	Normal boiling point	Critical point
Methane	90.7	111.6	190.5
Oxygen	54.4	90.2	154.6
Argon	83.8	87.3	150.9
Nitrogen	63.1	77.3	126.2
Neon	24.6	27.1	44.4
Hydrogen	13.8	20.4	33.2
Helium	2.2*	4.2	5.2

*Lambda point

The useful range of cryogens for cooling equipment is essentially in liquid form when one can make use of the latent heat of vaporisation, i.e. from the triple point up to the critical point. Exceptionally, cryogens—particularly helium—can be used in the supercritical domain, but the temperature is then no longer fixed by a mono-variant thermodynamic state.

This chapter should be cited as: Cryogenics for superconducting device, Ph. Lebrun, DOI: 10.23730/CYRSP-2024-003.1243, in: Proceedings of the Joint Universities Accelerator School (JUAS): Courses and exercises, E. Métral (ed.), CERN Yellow Reports: School Proceedings, CERN-2024-003, DOI: 10.23730/CYRSP-2024-003, p. 1243.

Comparing the useful range of liquid cryogens with the critical temperature of some practical superconductors (see Fig. II.7.1), and remembering that superconductors should be operated at a fraction of their critical temperature, one can see that helium and nitrogen are the cryogens of choice for low- and high-temperature superconductors, respectively. Hydrogen and neon are seldom used, the first due to its flammability and the second in view of its high cost. In the following, we will therefore concentrate on helium and nitrogen.

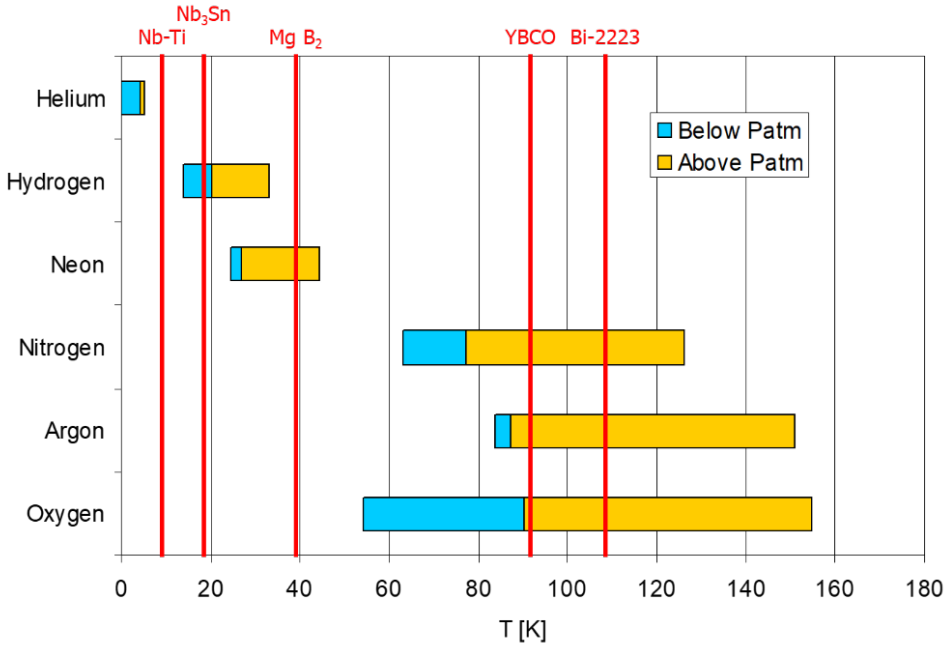

Fig. II.7.1: Useful range of cryogens for cooling superconductors.

II.7.2 Cryogenic fluids

To develop a feeling for the basic properties of liquid helium and liquid nitrogen, it is useful to compare them to a common, well-known fluid: water (see Table II.7.1).

Table II.7.1: Properties of cryogens compared to water.

Property	Helium	Nitrogen	Water
Normal boiling point (K)	4.2	77	373
Critical temperature (K)	5.2	126	647
Critical pressure (K)	2.3	34	221
Liquid/vapour density ratio at NBP	7.4	175	1600
Heat of vaporisation at NBP ($J.g^{-1}$)	20.4	199	2260
Liquid viscosity at NBP (μPl)	3.3	152	278

A first observation is that the normal boiling point (NBP) of helium is close to the critical point: there is little difference between liquid and vapour and the heat of vaporisation—difference in enthalpy

between the liquid and vapour phases—is low. The same is true, to a lesser extent for nitrogen. Consequently, helium will be easily vaporized by heat in-leaks to a cryogenic system.

A one-W heat in-leak will vaporize 1.38 L/h of helium, producing 16.4 L/min NTP (normal temperature and pressure) of vapour. The corresponding values for nitrogen are only 0.02 L/h and 0.24 L/min NTP. Two consequences can be drawn from this: i) it is essential to optimize the thermal insulation of liquid helium vessels, and ii) liquid nitrogen can provide an effective and economical solution for intercepting heat in-leaks before they reach the liquid helium.

Liquid helium shows a low viscosity, suitable to permeate the windings of superconducting magnets for their thermal stabilization. This can be very efficient in view of the strong decrease in specific heat of solid materials at low temperature, typically four orders of magnitude lower than helium at 4.2 K, as shown in Fig. II.7.1. Thus, even a small amount of helium in good thermal contact with a superconducting winding provides an effective thermal buffer as it concentrates most of the sensible heat of the superconductor + helium compound assembly: this is the basis of the so-called cryogenic stabilization of superconductors.

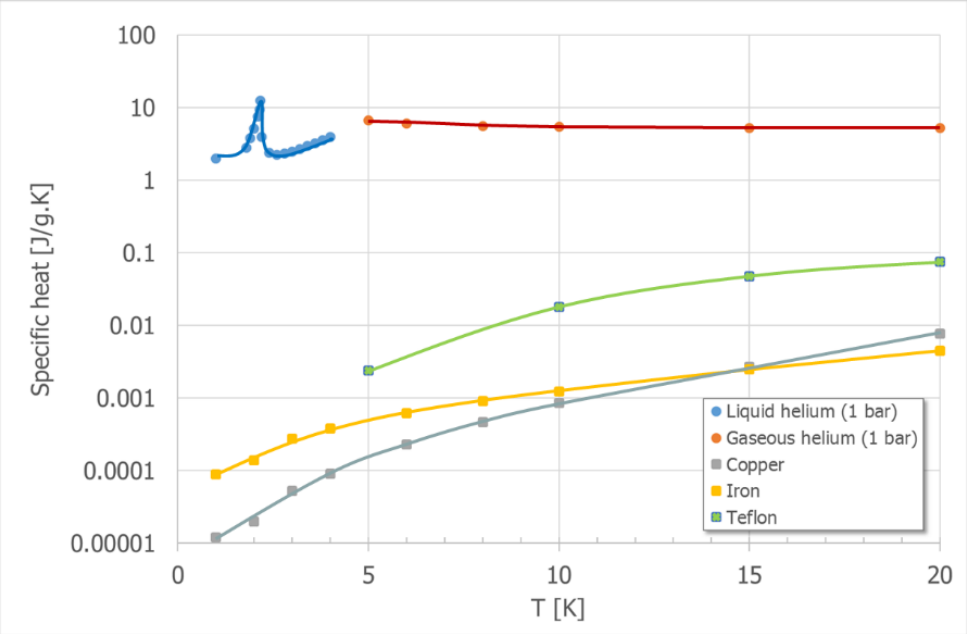

Fig. II.7.1: Specific heat of helium and solid materials.

The amount of cryogen required for cooling down solid materials, e.g. iron, from T_{initial} to T_{final}, assuming perfect heat exchange between the solid and the cryogen, is given by the enthalpy balance equation

$$\int_{T_{\text{final}}}^{T_{\text{initial}}} M_{\text{Fe}}\, C_{\text{Fe}}\, dT \;=\; m\,[L_{\text{v}} \,+\, (h_{\text{vap}}^{\text{final}} \,-\, h_{\text{vap}}^{\text{sat}})] \;\approx\; m\,[\,L_{\text{v}} \,+\, C_{\text{p}}\,(T_{\text{final}} - T_{\text{sat}})] \quad , \tag{1}$$

where M_{Fe} and C_{Fe} are the mass and specific heat of iron, L_{v} and C_{p} are the latent heat of vaporization and the specific heat of the cryogen, respectively, and $h_{\text{vap}}^{\text{sat}}$ and $h_{\text{vap}}^{\text{final}}$ are the values of enthalpy of the

cryogen vapour at saturation and at the final temperature, respectively. The results (see Table II.7.2) lead to two important practical consequences for minimizing liquid helium consumption. First, one should definitely make the best possible use of the cooling capacity of the cold helium vapour by ensuring its good heat exchange with the object to be cooled. Second, liquid nitrogen should be used whenever possible for pre-cooling down to about 80 K.

Table II.7.2: Amount of cryogens (L) required to cool down 1 kg of iron.

Using	**Latent heat only**	**Latent heat and enthalpy of vapour**
Liquid helium from 290 K to 4.2 K	29.5	0.75
Liquid helium from 77 K to 4.2 K	1.46	0.12
Liquid nitrogen from 290 K to 77 K	0.45	0.29

II.7.3 Refrigeration and liquefaction

The First Principle of thermodynamics expresses energy conservation. For a given thermodynamic system

$$Q + W = \Delta U + \Delta K \quad , \tag{2}$$

where Q and W are the heat and work received by the system, respectively, ΔU is the change in internal energy of the system, and ΔK is the change in macroscopic kinetic energy of the system. In refrigeration this latter term is usually negligible in comparison with the others. This equation is a macroscopic definition of internal energy (within an additive constant).

For a system of microscopic particles, internal energy U can also be defined as

$$U = \sum E_{\text{kin,micro}}(T) + \sum E_{\text{pot,micro}} \quad , \tag{3}$$

where $\sum E_{\text{kin,micro}}(T)$ is the sum of kinetic energies of particles in the system (an increasing function of temperature) and $\sum E_{\text{pot,micro}}$ is the sum of potential energies of particles in the system. Note that by definition this latter term, which represents the interaction between particles, is nil for an ideal gas.

To reduce the temperature of a gas, one needs to lower $\sum E_{\text{kin,micro}}(T)$. This can be done by removing heat Q from the gas (e.g. in a heat exchanger with a colder fluid), or by removing work W (e.g. by expanding the gas with extraction of motor work in a piston engine or a turbine). At constant internal energy, it can also be done by increasing $\sum E_{\text{pot,micro}}$, expanding the gas without extraction of motor work in a valve (Joule-Thomson expansion). This latter process is interesting in view of the simplicity of technical equipment required. It however works only for non-ideal gases and in a limited temperature domain, below the so-called inversion temperature of the gas (see Table II.7.1).

For cryogenic helium refrigeration and liquefaction, these three cooling processes are usually combined in a Claude cycle (see Figure II.7.1). The high-pressure (15 to 20 bar) gas stream supplied to the “cold box” is first cooled by expansion in turbines and heat exchange with the returning low-pressure stream, down to a temperature well below the inversion temperature. It is then finally expanded and

Table II.7.1: Maximum inversion temperatures of cryogenic gases.

Cryogen	Maximum inversion temperature (K)
Oxygen	761
Nitrogen	623
Air	603
Neon	260
Hydrogen	202
Helium	43

liquefied in a Joule-Thomson valve. Seeking high efficiency, large-capacity helium refrigerators use more complex Claude-type cycles, with numerous heat exchangers and turbines. The final expansion stage may also be done in a "wet" turbine instead of the Joule-Thomson valve, resulting in higher liquefaction rate.

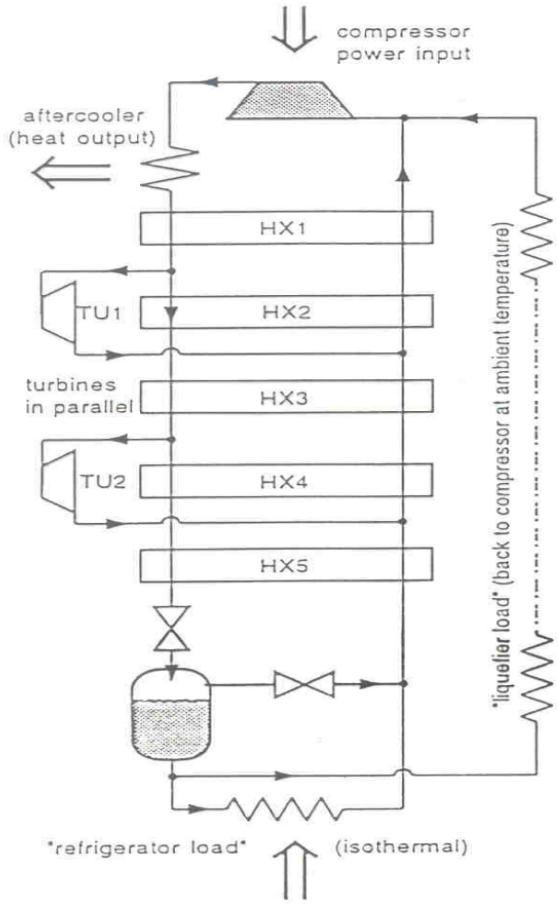

Fig. II.7.1: A simple Claude cycle for helium refrigeration and liquefaction.

The Second Principle of thermodynamics expresses that mechanical work W is required to extract heat Q_{i} at low temperature T_{i} and reject it at room temperature T_0, with $T_{\mathrm{i}} < T_0$: this is the basis of refrigeration (see Figure II.7.2). The First Principle (conservation of energy) leads to

$$Q_0 = Q_\mathrm{i} + W \quad , \tag{4}$$

while the Second Principle (Clausius formulation) writes

$$\frac{Q_0}{T_0} \geq \frac{Q_\mathrm{i}}{/T_\mathrm{i}} \quad , \tag{5}$$

where the equal sign applies in the case of a reversible process. Combining the above equations, one gets

$$W \geq Q_\mathrm{i} \left(\frac{T_0}{T_\mathrm{i}} - 1 \right) \quad , \tag{6}$$

in which the term $T_0/T_\mathrm{i} - 1$, expressing the ratio of refrigeration work to heat extracted, is called the Carnot factor.

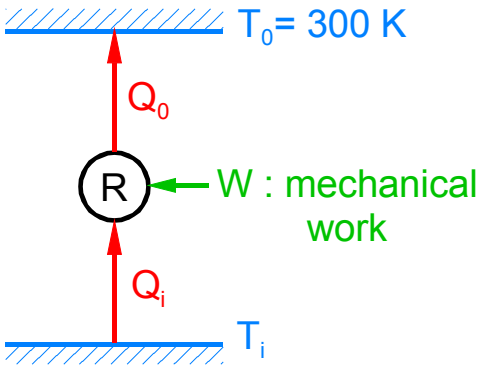

Fig. II.7.2: Thermodynamics of refrigeration.

As an example, consider the extraction of 1 W at liquid helium temperature 4.5 K, rejected at room temperature 300 K. The minimum refrigeration work, i.e. that of a Carnot refrigerator with no irreversibility, is

$$W_\mathrm{min} = Q_\mathrm{i} \left(\frac{T_0}{T_\mathrm{i}} - 1 \right) = 1 \left(\frac{300}{4.5} - 1 \right) \cong 65.7 \ \mathrm{W/W} \quad . \tag{7}$$

In practice, the most efficient helium refrigerators have an efficiency η of about 30 % with respect to the Carnot limit

$$W_\mathrm{real} = \frac{W_\mathrm{min}}{\eta} = \frac{65.7}{0.3} \cong 220 \ \mathrm{W/W} \quad . \tag{8}$$

As can be seen from Figure II.7.1, the cooling duty of a liquefier is higher than that of a refrigerator of equal flow-rate, since the low-pressure gas stream is returned at room temperature to the compressor, and its cooling power therefore not recovered in the heat exchange line. For helium, an approximate capacity equivalence is 100 W refrigeration at 4.2 K for 1 g s^{-1} liquefaction. One should however keep in mind that this equivalence is solely based on thermodynamics, and that the corresponding pieces of machinery, refrigerator or liquefier, show important differences in design and construction.

II.7.4 Heat transfer and thermal insulation

Knowing the processes and laws of heat transfer at low temperatures is essential in cryogenic design, whether one wishes to maximize heat transfer, e.g. for efficient cooling of the superconducting device, or to minimize it, e.g. for improving the thermal insulation of its cryostat and thus reduce the refrigeration duty. While the thermal processes at work are the same as at room temperature, at low temperature they show very different magnitudes as well as non-linear behaviour. In many cases, the superconducting device is immersed in a bath of cryogen at saturation (see Table II.7.1) and cooled by pool boiling, a typical example of non-linear heat transfer. Figure II.7.1 shows the heat transfer characteristic of pool boiling in liquid nitrogen. At low heat flux prevails the efficient regime of nucleate boiling: the vapour bubbles nucleate independently on the heated surface and rise to evacuate the heat. This regime peaks when the bubbles are so numerous that they start interacting with each other ("boiling crisis"), reaching the so-called peak nucleate boiling flux (PNBF). At higher heat flux, the heat transfer drops by an order of magnitude as film boiling develops: the heated surface is covered by a uniform layer of vapour and the superheat of the surface shoots up. Moreover, this transition shows hysteresis, so that nucleate boiling can only be recovered by lowering substantially the applied heat flux. Consequently, bath-cooled superconducting devices must be operated in the nucleate boiling regime.

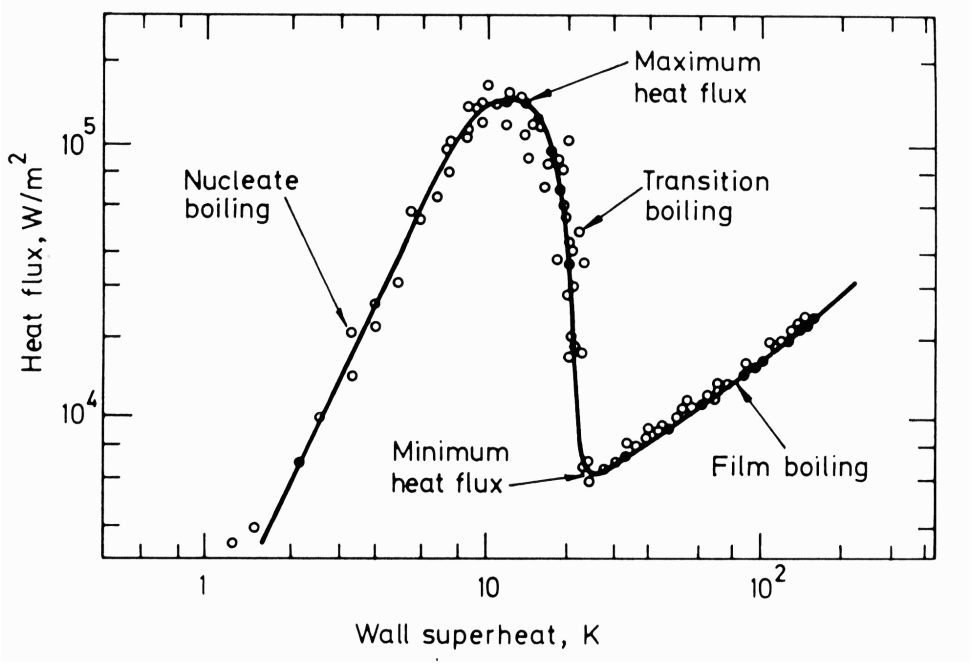

Fig. II.7.1: Pool boiling heat transfer of liquid nitrogen.

For liquid nitrogen at the normal boiling point, the PNBF is $1.5 \times 10^5\,\mathrm{W\,m^{-2}}$ with a wall superheat of about 10 K. A similar curve can be established for liquid helium at the normal boiling point, showing a PNBF of $10^4\,\mathrm{W\,m^{-2}}$ and a corresponding wall superheat of about one K: in nucleate boiling, the surface temperature of a superconductor cooled in saturated helium at 4.2 K is less than one K above that of the bath.

Thermal conduction in solids is at work in numerous cases, whether one wishes to limit heat transfer, as in cold mass support struts, or improve it, as in thermal links or across electrical insulation of the conductors. In the one-dimensional case, conductive heat transfer across a cross-section A is represented by Fourier's law

$$\dot{Q}_{\text{cond}} = k(T)\, A\, \frac{dT}{dx} \quad , \tag{9}$$

where $k(T)$ is the thermal conductivity of the material, particularly dependent on temperature in the cryogenic domain. Calculating conduction along a rod of uniform cross-section A and length L with its ends kept at temperatures T_1 and T_2 therefore requires integration

$$\dot{Q}_{\text{cond}} = \frac{A}{L} \int_{T_1}^{T_2} k(T)\, dT \quad . \tag{10}$$

To simplify the calculation, tables of thermal conductivity integrals are available for the cryogenic temperature domain. Table II.7.1 shows large variations in conductivity among materials, from metals and, to a less extent alloys (good or medium conductors) to non-metallic materials (insulators). Comparison between OFHC and DHP copper illustrates the dependence on metal purity, while the decrease of conductivity integrals with decreasing temperature hints towards the importance of heat interception at some intermediate point. As an example, the thermal conductivity integral of austenitic stainless steel AISI 304 from 80 K is an order of magnitude lower than that from 290 K: an intermediate 80 K heat sink on a stainless-steel support strut operating between 290 K and liquid helium thus allows strong reduction in the corresponding heat in-leak.

Table II.7.1: Thermal conductivity integrals of selected materials ($\mathrm{W\,m^{-1}}$).

From vanishingly low temperature up to	**20 K**	**80 K**	**290 K**
OFHC copper	11000	60600	152000
DHP copper	395	5890	46100
1100 aluminium	2740	23300	72100
2024 aluminium alloy	160	2420	22900
AISI 304 stainless steel	16.3	349	3060
G-10 glass-epoxy composite	2	18	153

Low-pressure gas conduction is at work in the so-called "vacuum" insulation spaces of cryostats and cryogenic transfer lines (in fact filled with residual gases), therefore playing an important role in thermal insulation (and conversely in parasitic heat in-leaks!). Two different regimes apply, depending upon the relative values of the mean free path of the molecules $\lambda_{\text{molecule}}$ and of the heat transfer distance d.

At higher pressure, $\lambda_{\text{molecule}} \ll d$ and the viscous regime prevails, with a classical conduction law

$$\dot{Q}_{\text{residual}} = A\, k(T)\, \frac{dT}{dx} \quad , \tag{11}$$

with the thermal conductivity $k(T)$ depending on the nature of the gas, but not on its residual pressure.

At lower pressure, $\lambda_{\text{molecule}} \gg d$ and the molecular regime prevails. The conductive heat transfer between plates at temperatures T_1 and T_2 then follows Kennard's law

$$\dot{Q}_{\text{residual}} = A\,\alpha(T)\,\Omega\,P\,(T_2 - T_1) \quad , \tag{12}$$

where the parameter Ω depends on the gas species, and the accommodation coefficient $\alpha(T)$ depends on T_1, T_2 and the gas species. Note that in the molecular regime, the heat transfer is proportional to the temperature difference and to the residual pressure, and independent on the spacing between the plates. Consequently one cannot define a thermal conductivity in the sense of Fourier's law.

Thermal radiation is a heat transfer process which does not need a material medium: it is therefore the prevailing process in the evacuated insulation spaces of cryogenic equipment. Black-body radiation follows Stefan-Boltzmann's law

$$\dot{Q}_{\text{rad}} = \sigma\,A\,T^4 \quad , \tag{13}$$

with $\sigma = 5.67 \times 10^{-12}$ W m^{-2} K^{-4}. Note the fourth-power dependence on absolute temperature, which favors the use of thermal screens cooled at intermediate temperature to reduce radiative heat in-leak to the inner vessels of cryostats. Technical surfaces are usually modelled as "gray" bodies, characterized by a surface emissivity ϵ comprised between 0 and 1. The heat radiated is then

$$\dot{Q}_{\text{rad}} = \epsilon\,\sigma\,A\,T^4 \quad . \tag{14}$$

Radiative heat transfer between surfaces at temperature T_1 and T_2 is given by

$$\dot{Q}_{\text{rad}} = E\,\sigma\,A\,(T_2^4 - T_1^4) \quad , \tag{15}$$

with the emissivity factor E depending upon the geometry of the facing surfaces, their emissivities ϵ_1 and ϵ_2 and the type of reflectivity (specular or diffuse). As an indication, some values of emissivity for technical surfaces are listed in Table II.7.2.

Heat transfer by thermal convection, i.e. macroscopic flow in cryogenic fluids follows the same laws as at higher temperatures, and the correlations established for "normal" fluids generally apply. A particular mention should be made of natural convection, driven by buoyancy of a fluid encountering differences in temperature. In view of the high volume expansivity of gases at low temperature, large density gradients can appear, driving very strong convection currents. This is particularly true for helium vapour and can be used for homogenising temperature inside a helium container.

A compound insulation system of frequent use in cryogenic systems is multi-layer reflective insulation (MLI), composed of a stack of reflective layers (aluminium-coated plastic film) spaced by low-conduction sheets minimizing contacts, and evacuated. Heat transfer across a MLI blanket can be written

Table II.7.2: Emissivity of technical materials at low temperature.

	Radiation from a 290 K Surface to 77 K	**Radiation from a 77 K Surface to 4.2 K**
Stainless steel, as found	0.34	0.12
Stainless steel, mechanically polished	0.12	0.07
Stainless steel, electropolished	0.10	0.07
Stainless steel + aluminium foil	0.05	0.01
Aluminium, as found	0.12	0.07
Aluminium, mechanically polished	0.10	0.06
Aluminium, electropolished	0.08	0.04
Copper, as found	0.12	0.06
Copper, mechanically polished	0.06	0.02

$$\dot{Q}_{\text{MLI}} = \dot{Q}_{\text{rad}} + \dot{Q}_{\text{contact}} + \dot{Q}_{\text{residual}} \quad . \tag{16}$$

With n reflective layers of equal emissivity, $\dot{Q}_{\text{rad}} \approx 1/(n+1)$. Provided one operates in molecular regime between layers, $\dot{Q}_{\text{residual}}$ scales as $1/n$. This pushes towards increasing the number of layers. However, due to parasitic contacts between layers, $\dot{Q}_{\text{contact}}$ increases with layer density, which also increases with n, given an overall thickness of the blanket. In practice, typical heat transfer data across MLI is available from an abundant literature. For particular cases, performance can be measured on test samples. To be reflective in the infrared spectrum of thermal radiation (peaking at 10 μm for 290 K versus 0.6 μm for visible light), the aluminium layer deposited on the plastic film must be much thicker than the electromagnetic penetration depth of the radiation; in practice a thickness of several hundred Å is required. This can be checked by electrical resistance measurements on a sample.

Typical heat flux between flat plates, one of which is kept at vanishing low temperature, is given for indicative purpose in Table II.7.3.

Table II.7.3: Typical heat fluxes at vanishingly low temperature between flat plates (W m^{-2}).

Process	**Heat flux**
Black-body radiation from 290 K	401
Black-body radiation from 80 K	2.3
Gas conduction (100 mPa He) from 290 K	19
Gas conduction (1 mPa He) from 290 K	0.19
Gas conduction (100 mPa He) from 80 K	6.8
Gas conduction (1 mPa He) from 80 K	0.07
MLI (30 layers) from 290 K, pressure below 1 mPa	1.0 – 1.5
MLI (10 layers) from 80 K, pressure below 1 mPa	0.05
MLI (10 layers) from 80 K, pressure 100 mPa	1 – 2

II.7.5 Thermal screening with cold vapour

By virtue of Nernst's Principle, the latent heats of vaporization of cryogens decrease with decreasing temperature, while the specific (sensible) heats of their vapours remain finite (and even constant in the range they approximate the ideal gas). The boil-off vapour from a liquid cryogen bath therefore contains still an important cooling capacity in comparison with the heat of vaporization of the liquid, and can provide heat interception and thermal screening, thus reducing the heat in-leak to the bath. This is the principle of vapour cooling of cryostat neck and supports.

Consider a solid thermal conductor (a support strut or a cryostat neck) with the bottom dipping in a liquid cryogen bath and the top at some higher temperature, cooled by a return flow $\dot{m}$ of cold vapour from the bath (see Figure II.7.1).

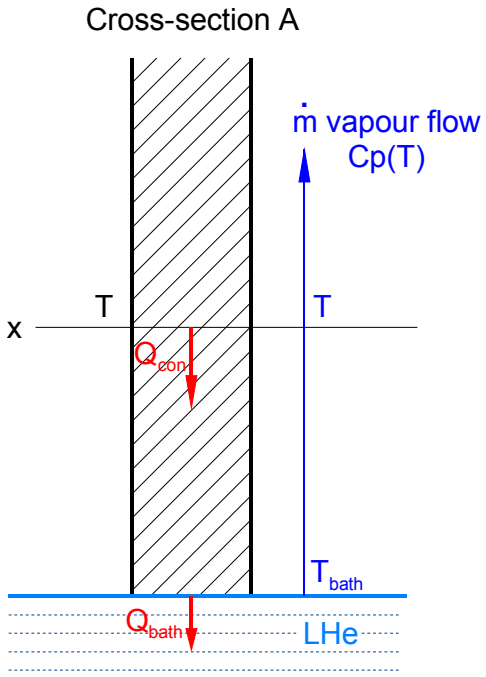

Fig. II.7.1: Thermodynamics of refrigeration.

Assuming perfect heat exchange between solid and vapor, i.e. $T_{\text{solid}}(x) = T_{\text{vapour}}(x) = T(x)$, the steady-state heat balance below level x yields

$$\dot{Q}_{\text{cond}} = \dot{Q}_{\text{bath}} + \dot{m}\, C_{\text{p}}(T)\,(T - T_{\text{bath}}) \quad , \tag{17}$$

$$A\, k(T) \frac{dT}{dx} = \dot{Q}_{\text{bath}} + \dot{m}\, C_{\text{p}}(T)\,(T - T_{\text{bath}}) \quad , \tag{18}$$

where $k(T)$ and $C_{\text{p}}(T)$ are the thermal conductivity of the solid and the specific heat of the vapour, respectively. From this equation, $\dot{Q}_{\text{bath}}$ can be calculated by numerical integration for different cryogens, different values of the aspect ratio of the solid and different values of the vapour flow.

A particular case of vapour cooling is the self-sustained mode, in which the vapour flow is pre-

cisely the boil-off generated by the residual heat $\dot{Q}_{\text{bath}}$ reaching the bath

$$\dot{Q}_{\text{bath}} \;=\; L_{\text{v}}\,\dot{m} \quad , \tag{19}$$

where L_{v} is the latent heat of vaporization of the liquid cryogen. The variables can then be separated and analytic integration of the heat balance equation yields

$$\dot{Q}_{\text{bath}} = \frac{A}{L}\int_{T_{\text{bath}}}^{T} \frac{k(T)}{1+\frac{C_{\text{p}}(T)}{L_v}(T-T_{\text{bath}})}\,dT \quad . \tag{20}$$

The denominator of the integrand $1+\frac{C_{\text{p}}(T)}{L_v}(T-T_{\text{bath}})$ acts as an attenuation factor of the thermal conductivity $k(T)$. Over integration, this attenuation can be up to an order of magnitude, as can be seen from Table II.7.1.

Table II.7.1: Reduction of heat conduction into liquid helium by self-sustained helium vapour cooling (W cm^{-1}).

Effective conductivity integral (300 K to 4 K)	**Pure conduction**	**Self-sustained vapour cooling**
ETP copper	1620	128
OFHC copper	1520	110
1100 aluminium	728	39.9
Nickel 99 % pure	213	8.65
Constantan	51.6	1.94
AISI 300 stainless steel	30.6	0.92

In the previous case, the vapour flow intercepts the largest part of the conductive heat in-leak in the solid. Additionally, if this solid is the seat of heat dissipation, e.g. by Joule heating, vapour cooling can also help limiting the heat flow to the liquid bath. This is the principle of vapour-cooled current leads bringing electrical current from room temperature into the bath housing a superconducting magnet (see Figure II.7.2).

If the solid conductor, of electrical resistivity $\rho(T)$, carries a current I, the steady-state heat balance equation becomes

$$\frac{d}{dx}\left[A\,k(T)\,\frac{dT}{dx}\right] \;-\; \dot{m}\,C_{\text{p}}(T)\frac{dT}{dx} \;+\; \frac{\rho(T)I^2}{A} \;=\; 0 \quad . \tag{21}$$

Integration of this equation is difficult as its parameters $k(T)$, $\rho(T)$ and to some extent $C_{\text{p}}(T)$ all depend on temperature, with large variations in the domain of interest. It can however be simplified if one considers that the solid conductor is made of a metal following the Wiedemann-Franz-Lorentz (WFL) law, which relates $k(T)$, $\rho(T)$ and T

$$k(T)\rho(T) \;=\; \mathcal{L}_0\,T \quad , \tag{22}$$

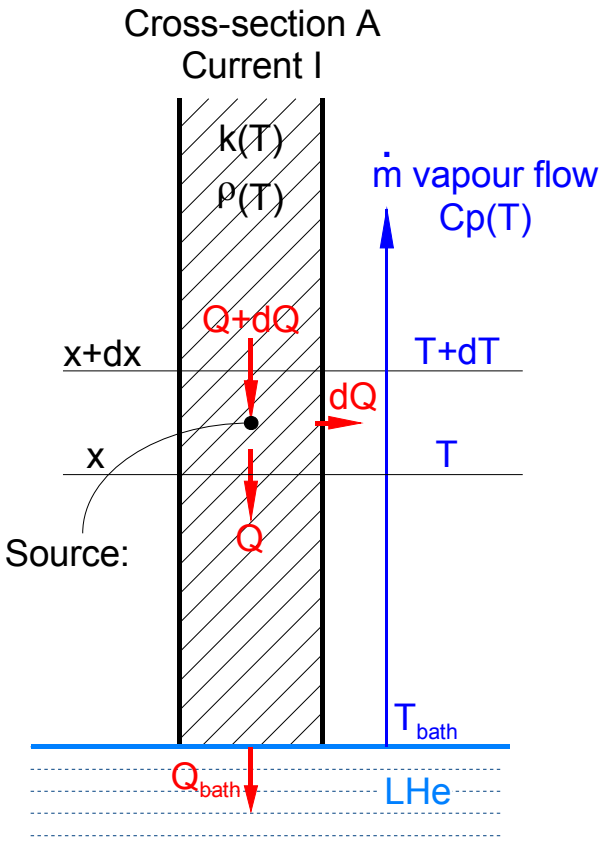

Fig. II.7.2: Vapour-cooled current lead.

with $\mathcal{L}_0 = 2.45 \times 10^{-8}\,\mathrm{W\,\Omega\,K^{-2}}$. The WFL law, simply expressing that good electrical conductors are also good thermal conductors, is well followed by pure metals, e.g. electrical-grade copper. Solving the heat balance equation in that particular case, one can show that whatever the material, the aspect ratio L/A of the solid conductor can be chosen for minimizing the heat in-leak $\dot{Q}_{\mathrm{bath}}$; that minimum heat in-leak does not depend on the material and is equal to $1.04\ \mathrm{W\,k\,A^{-1}}$.

Reducing the heat in-leak beyond that limit requires using a material not following the WFL law, e.g. an alloy or better, a superconductor, which shows bad thermal conductivity and nil electrical resistivity. In the absence of room-temperature superconductors, such a solution may only be implemented up to a maximum temperature of operation in the superconducting state, i.e. a fraction of the critical temperature. Several hundred current leads, built with a "high-temperature" superconductor in the lower part (up to about 50 K), and a vapour-cooled copper conductor in the upper part (up to room temperature), are currently operating in the Large Hadron Collider at CERN. The residual heat reaching the helium bath is reduced by an order of magnitude, and the total refrigeration duty (including the cooling of the upper part) by a factor three.

II.7.6 Summary

This brief overview of cryogenics applicable to the cooling of superconducting devices aims only at presenting the basic processes, giving the correct orders of magnitude, and alerting the system designer

to some possible pitfalls. A lot more, that can be found in the bibliography and references listed below, is required to address and solve all issues of a real project. Should a single idea be retained from this course, it is that, for the sake of functionality, efficiency and finally success, cryogenics should be integrated from the onset into the design of a superconducting device.

II.7.7 Bibliography

- K. Mendelssohn, The quest for absolute zero, McGraw Hill (1966).
- R.B. Scott, Cryogenic engineering, Van Nostrand, Princeton (1959).
- G.G. Haselden, Cryogenic fundamentals, Academic Press, London (1971).
- R.A. Barron, Cryogenic systems, Oxford University Press, New York (1985).
- B.A. Hands, Cryogenic engineering, Academic Press, London (1986).
- S.W. van Sciver, Helium cryogenics, Plenum Press, New York (1986, 2nd edition 2012),doi:10.1007/978-1-4419-9979-5.
- K.D. Timmerhaus and T.M. Flynn, Cryogenic process engineering, Plenum Press, New York (1989).
- J.G. Weisend (ed.), The handbook of cryogenic engineering, Taylor and Francis, Philadelphia (1998).
- J.G. Weisend (ed.), Cryostat design: case studies, principles and engineering, Springer, Switzerland (2016), doi:10.1007/978-3-319-31150-0.

References

[1] Ph. Lebrun, An introduction to cryogenics, CERN-AT-2007-01 (CERN, Geneva, 2007), doi:10.17181/CERN.KOEP.SD6C.

[2] U. Wagner, Refrigeration, in CERN Accelerator School: Superconductivity and Cryogenics for Accelerators and Detectors, 8–17 May 2002, Erice, Italy, Eds. S. Russenschuck and G. Vandoni(CERN, Geneva, 2004), pp. 295–345, doi:10.5170/CERN-2004-008.295.

[3] G. Vandoni, Heat transfer, in CERN Accelerator School: Superconductivity and Cryogenics for Accelerators and Detectors, 8–17 May 2002, Erice, Italy, Eds. S. Russenschuck and G. Vandoni(CERN, Geneva, 2004), pp. 325–345, doi:10.5170/CERN-2004-008.325.

[4] Ph. Lebrun, Design of a cryostat for superconducting accelerator magnet, in CERN Accelerator School: Superconductivity and Cryogenics for Accelerators and Detectors, 8–17 May 2002, Erice, Italy, Eds. S. Russenschuck and G. Vandoni(CERN, Geneva, 2004), pp. 348–361, doi:10.5170/CERN-2004-008.348.

[5] Ph. Lebrun and L. Tavian, The technology of superfluid helium, in CERN Accelerator School: Superconductivity and Cryogenics for Accelerators and Detectors, 8–17 May 2002, Erice, Italy, Eds. S. Russenschuck and G. Vandoni(CERN, Geneva, 2004), pp. 375–389, doi:10.5170/CERN-2004-008.375.

[6] P. Duthil, Basic thermodynamics, in CERN Accelerator School: Course on Superconductivity for Accelerators (CAS 2013), 24 April–4 May 2013, Erice, Italy, Ed. R. Bailey (CERN, Geneva, 2014), pp. 1–20, doi:10.5170/CERN-2014-005.1.

[7] P. Duthil, Material properties at low temperatures, in CERN Accelerator School: Course on Superconductivity for Accelerators (CAS 2013), 24 April–4 May 2013, Erice, Italy, Ed. R. Bailey (CERN, Geneva, 2014), pp. 77–95, doi:10.5170/CERN-2014-005.77.

[8] A. Alekseev, Basics of low-temperature refrigeration, in CERN Accelerator School: Course on Superconductivity for Accelerators (CAS 2013), 24 April–4 May 2013, Erice, Italy, Ed. R. Bailey (CERN, Geneva, 2014), pp. 111–139, doi:10.5170/CERN-2014-005.111.

[9] B. Baudouy, Heat transfer and cooling techniques at low temperature, in CERN Accelerator School: Course on Superconductivity for Accelerators (CAS 2013), 24 April–4 May 2013, Erice, Italy, Ed. R. Bailey (CERN, Geneva, 2014), pp. 329–352, doi:10.5170/CERN-2014-005.329.

[10] V. Parma, Cryostat design, in CERN Accelerator School: Course on Superconductivity for Accelerators (CAS 2013), 24 April–4 May 2013, Erice, Italy, Ed. R. Bailey (CERN, Geneva, 2014), pp. 353–399, doi:10.5170/CERN-2014-005.353.

[11] Ph. Lebrun and L. Tavian, Cooling with superfluid helium, in CERN Accelerator School: Course on Superconductivity for Accelerators (CAS 2013), 24 April–4 May 2013, Erice, Italy, Ed. R. Bailey (CERN, Geneva, 2014), pp. 453–476, doi:10.5170/CERN-2014-005.453.

[12] Proceedings of ICEC, CEC/ICMC and IIR Cryogenics conferences.